

Original Article

Economizing Generation Cost by Alleviating Congestion in DPS Employing FACTS Devices

Anubha Gautam¹, Rachna Dhir²

^{1,2}Department of Electrical Engineering, J.C. Bose University of Science and Technology, YMCA, Faridabad, Haryana, India.

²Corresponding Author : rachna@jcboseust.ac.in

Received: 04 January 2024

Revised: 03 February 2024

Accepted: 02 March 2024

Published: 25 March 2024

Abstract - The implementation of deregulation policies in modern power systems has intensified competition in the energy markets, introducing congestion in the system. This is a risk to the reliability and security of the system. In response to this challenge, one highly effective approach involves the rescheduling of generators, though at the cost of increased energy expenses. However, the emergence of Flexible AC Transmission System devices with the advancement of electronic power offers a promising opportunity to reduce the need for generator rescheduling significantly. FACTS devices assume a pivotal role in optimizing the overall power profile of the system by mitigating power losses. This research primarily focuses on the implementation of FACTS devices to curtail generation costs by alleviating congestion within the deregulated power system. Specifically, Static Var Compensators and Thyristor-Controlled Series Compensators are strategically integrated into the system to mitigate overloading. To identify the optimal locations for applied FACTS devices and fine-tune their parameters, we propose employing the teaching learning-based optimization algorithm. This approach aims to maximize the effectiveness of these devices. To validate the efficacy of the applied approach, SVC and TCSC are integrated into the IEEE 30 Bus system. Subsequently, a detailed comparison is conducted against Grey Wolf Optimization, which is documented in the existing literature, allowing us to verify the results and assess their significance.

Keywords - Deregulation, Flexible AC Transmission Systems, Congestion mitigation, Teaching Learning Based Optimization, Generation cost.

1. Introduction

1.1. Motivation

The escalating power needs of modern society, incited by technological progress and population growth, have brought a new era of power system deregulation. This shift has paved the way for private market players to step in, generating and supplying power to contracted consumers in the system. To fulfil the surging power demand, these generators rely on the existing transmission lines. Nevertheless, as these lines become increasingly overloaded, their capacity to transmit power efficiently diminishes. This, in turn, results in a rise in power losses throughout the system and a gradual deterioration of the system's reliability [1].

Laying more transmission lines to address losses faces challenges due to geographical and economic restrictions. As a result, a promising and rapidly evolving solution in the field of advanced power electronics, termed Flexible AC Transmission Systems (FACTS), is being incorporated into the existing framework. These devices serve a dual purpose: reducing system overloading and curbing power losses without burdening generators. The integration of FACTS

devices into the grid comes at a substantial cost. To maximize cost-effectiveness, it is essential to deploy FACTS at suitably optimized locations [2] strategically.

The application of FACTS represents a highly efficient and economical strategy for mitigating congestion caused by overloaded transmission lines. FACTS devices act proficiently in changing line reactance, controlling voltage levels at different buses, supplying both active and reactive power, and adjusting voltage angles at various bus locations [3]. System congestion impacts voltage magnitudes at various buses. The FACTS technology significantly contributes to improving the voltage profile of the system [4].

For sustained power supply without voltage disruptions, either reactive power demand should be reduced, or sufficient reactive power must be injected into the system before it reaches a critical voltage failure point [5]. For safety and cost-effectiveness, the implementation of FACTS devices is carried out with precision within the system [6]. A sensitivity factor-based approach is proposed in the literature to locate FACTS devices in congested systems.



In [7], an approach rooted in DCPTDF is suggested and verified using the IEEE 30 bus and six bus systems. It aims to mitigate congestion by boosting the system's Available Transfer Capacity (ATC). Line outage sensitivity factors are proposed in [8] for locating a series of FACTS devices to alleviate congestion in IEEE 14 and IEEE 57 bus systems. Line loss sensitivity indices and Total system loss sensitivity indices are proposed in [9].

Locational marginal price difference is used as a sensitivity factor in [10] to locate FACTS devices in IEEE 14, 30, and 57 bus systems for reducing congestion. In addition to sensitivity factor-based approaches, the literature also presents bio-inspired algorithms as an alternative method for locating FACTS devices. The essential advantage of employing these algorithms over sensitivity factor-based methods is their ability to determine device placements in real time, even in the presence of dynamic contingencies, faults, or changing hourly operational conditions

1.1. Research Gap

A comprehensive suite of cutting-edge methods is expertly employed to optimize the placement of FACTS devices for optimal performance. These methods encompass genetic algorithms, swarm optimization techniques, Sequential Ordering Learning (SOL) algorithms, differential evolution algorithms, and simulated annealing. Collectively, these methodologies enhance the precision of FACTS device positioning, strategically positioning them for maximum effectiveness [11].

Different FACTS devices, such as TCSC and STATCOM [12], SVC [13], UPFC [14], IPFC [15], etc., are strategically deployed within the system to alleviate congestion, thereby minimizing voltage degradation and curbing power losses. Numerous algorithms are designed to determine the best position for FACTS. In the literature, Particle Swarm Optimization (PSO) is harnessed as a powerful tool to identify optimal locations for mitigating congestion within the IEEE 6Bus system [16].

An Artificial Bees Colony (ABC) algorithm is proposed in [17] to locate UPFC and is tested on IEEE 30 bus and IEEE 14 bus systems. The Whale Optimization Algorithm (WOA) is introduced as a method to optimize the objective value with precision by accurately determining the positions and sizes of FACTS devices within the IEEE 30 Bus system [18].

Another approach to alleviating system congestion involves the adjustment of active power generation schedules. While this method is effective, it is essential to note that it can lead to economic implications, as rescheduling often results in elevated generation expenses. These expenses can be reduced by employing FACTS devices together with the generator rescheduling.

Therefore, it can be inferred that strategically positioned FACTS devices offer the most significant potential for enhancing the system's cost-effectiveness and operational performance by reducing generation costs. Many assessment tools have been utilized in the past to serve this purpose, but the Optimal Power Flow (OPF) distinguishes itself as exceptionally well-suited for this task. Its remarkable ability to quantify both economic and technical benefits straightforwardly plays a crucial role in guiding investment decisions.

1.2. Contribution

This paper delves into the economic benefits of strategically deploying FACTS devices to maximize profitability over their operational lifespan. Within this research, we utilize SVC and TCSC in the IEEE 30 Bus power system to optimize various aspects, such as mitigating congestion, reducing power losses, and minimizing generation costs.

To validate the findings, we conduct a comparative analysis between the results obtained using the Teaching Learning-Based Optimization (TLBO) algorithm and those achieved with other state-of-the-art algorithms found in the existing literature. This paper does an extensive work on the following:

- A deregulated environment is replicated by introducing an N-1 contingency simulation.
- The TLBO algorithm is utilized to optimize the placement and parameter settings of SVC and TCSC devices in the IEEE 30 Bus system under congested conditions.
- The reduction of active and reactive power losses serves to mitigate congestion within the system.
- The cost of generator rescheduling is decreased efficiently by the deployment of the FACTS devices implementing the TLBO algorithm.

This document is organized as follows: Section 1 gives a detailed introduction to the research, section 2 offers a comprehensive overview of the FACTS modelling examined in this study, and section 3 delves into the proposed TLBO algorithm in depth.

In section 4, we provide a thorough elucidation of the objective function and associated constraints. Section 5 covers the discussion of the results obtained, and section 6 outlines the conclusions drawn from the study.

2. Modelling of FACTS Devices

The mathematical representation of active power flow between i^{th} and j^{th} buses is as follows:

$$P_{ij} = \frac{v_i v_j}{x} \sin(\delta_i - \delta_j) \quad (1)$$

In Equation 1, P_{ij} represents the true power flow between i^{th} and j^{th} buses, V_i and V_j denotes voltages and δ_i and δ_j are respective voltage angles at the i^{th} and j^{th} buses. X signifies the reactance between the i^{th} and j^{th} buses. In the context of operational analysis within an electrical network, the power flow between any pair of buses is intricately influenced by the interplay of voltage magnitudes, voltage angles, and the impedance connecting these buses. The modelling of Flexible Alternating Current Transmission System (FACTS) devices aligns with these fundamental parameters.

2.1. SVC Modelling

An SVC serves as a crucial FACTS component that operates alongside transmission lines. SVCs play a pivotal role in upholding voltage stability and optimizing the operational efficiency of electrical power systems. Their rapid capability to regulate reactive power levels enhances their value to grid operators and utility companies, thereby fostering a dependable and robust power supply infrastructure [19]. The schematic of SVC can be presented as below:

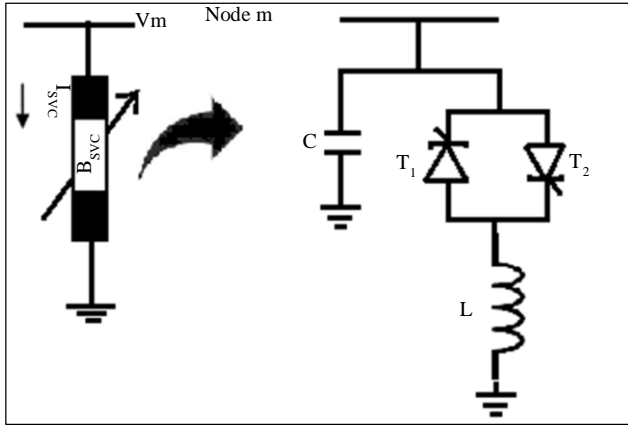


Fig. 1 Schematic of SVC

Figure 1 illustrates a thyristor-regulated reactor with a fixed capacitor. The expression for the current passing through the SVC can be formulated as follows:

$$I_{SVC} = jB_{SVC}V_{ref} \quad (2)$$

In Equation 2, I_{SVC} represents the current provided by the SVC, B_{SVC} denotes the susceptance of the SVC and V_{ref} denotes reference voltage at the bus (node m). The reactive power limitations of SVC can be given by:

$$Q_{max} = B_L \times V_{ref}^2 \quad (3)$$

$$Q_{min} = B_C \times V_{ref}^2 \quad (4)$$

In Equation 3 and 4, B_C & B_L and denotes the capacitive susceptance and inductive susceptance of SVC.

2.2. TCSC Modelling

The TCSC is a highly adaptable series FACTS device capable of efficiently adjusting line reactance as needed. Figure 2 represents the schematic of TCSC.

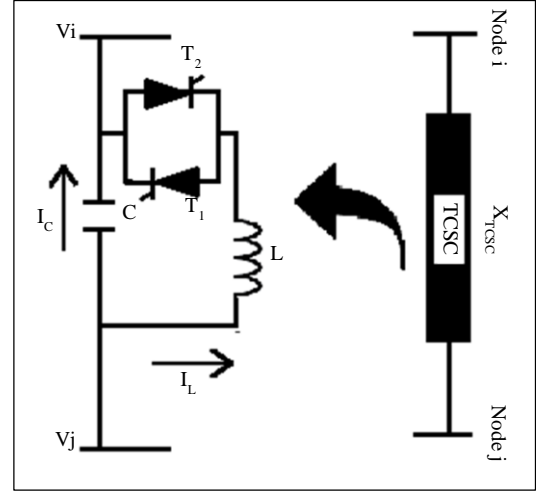


Fig. 2 Schematic of TCSC

Let Y_{ij} be the line admittance between i^{th} and j^{th} buses without placing TCSC; this can be mathematically represented as:

$$Y_{ij} = G_{ij} + jB_{ij} \quad (5)$$

When TCSC is implemented in the circuit, the change in admittance can be given as follows:

$$\Delta Y_{ij} = y'_{ij} - y_{ij} \quad (6)$$

$$\Delta Y_{ij} = \{(G'_{ij} + B'_{ij}) - (G_{ij} + B_{ij})\} \quad (7)$$

In Equation 7:

$$\left. \begin{aligned} G_{ij} &= \frac{R_{ij}}{\sqrt{R_{ij}^2 + X_{ij}^2}} \\ B_{ij} &= \frac{-X_{ij}}{\sqrt{R_{ij}^2 + X_{ij}^2}} \end{aligned} \right\} \quad (8)$$

and

$$\left. \begin{aligned} G'_{ij} &= \frac{R_{ij}}{\sqrt{R_{ij}^2 + (X_{ij} + X_{tcsc})^2}} \\ B_{ij} &= \frac{-(X_{ij} + X_{tcsc})}{\sqrt{R_{ij}^2 + (X_{ij} + X_{tcsc})^2}} \end{aligned} \right\} \quad (9)$$

With a modification in X_{tcsc} parameter, the line's total admittance is altered, and this modification is subsequently incorporated into the load flow analysis to determine the line flows.

3. Teaching Learning Based Optimization (TLBO)

This algorithm is based on the interactive connection between teachers and students, which is a fundamental aspect of how knowledge is shared in a classroom setting. TLBO is based on two primary phases: 'The Teachers' Phase and 'The Learners' Phase.'

In this framework, the size of the classroom represents the scope of exploration. The teacher's role in this process can be compared to that of an 'Influencer,' as they guide and mould the students to achieve successful learning outcomes. [20]. The two stages of the algorithm are:

3.1. Teacher Phase

During this phase, the teacher assumes a pivotal position in improving the student's achievements within the classroom setting. The teacher is responsible for sharing knowledge and information with the students, which makes this phase primarily centred around transferring knowledge from the teacher to the learners. It is presumed that the teacher has a greater level of knowledge and expertise, making them the primary source of information. As the simulation progresses, the highest-performing student will eventually take on the role of the teacher. This transition can be explained using a mathematical equation as follows (10):

$$D_n = rand[X_{teach} - T_f(X_n)] \quad (10)$$

In Equation 10, D_n signifies the difference in performance between teachers (X_{teach}) at their best and the current average performance of the learners, X_n . T_f is used to represent the teaching factor, and while its exact value isn't explicitly mentioned in the literature, better results can be obtained by using values between (1, 2). T_f can be calculated as follows:

$$T_f = round\{1 + rand [0,1](2 - 1)\} \quad (11)$$

$rand$ is a random value in the range of [0, 1]. The updated solution can be represented as in Equation 12:

$$X_{updated} = X_{existing} + D_n \quad (12)$$

In this step, the new value is employed to determine the updated fitness function value. If the current fitness value exceeds the previous one, the updated result is noted. These adjusted values serve as the initial input for the subsequent stage, which is referred to as the learning phase.

3.2. Learner Phase

In this phase, there is a group of learners who interact only with each other, with partners chosen at random. In this stage, the learner receives information and guidance from both the teacher and the partner they were randomly paired with.

The learner's understanding and skills can improve when their randomly selected partner happens to have more expertise than they do. Let's consider two learners X_1 and X_2 . The performance metrics for X_1 and X_2 are evaluated and then compared. Equation 13 is used to calculate updated values for the minimization function by the following equation:

$$\begin{aligned} X_{updated} &= X_{existing} + rand (X_1 - X_2) \\ X_{updated} &= X_{existing} + rand (X_2 - X_1) \end{aligned} \quad (13)$$

4. Problem Formulation

The expression describing the cost function for the generated active power can be formulated as follows:

$$C_{Pi} = \alpha_i + \beta_i P_{gi} + \gamma_i P_{gi}^2 \quad \$/hr \quad (14)$$

In Equation 15, C_{Pi} represents the cost of active power generation for i^{th} generator, α_i , β_i and γ_i represents the cost coefficient for i^{th} generator. So, calculating the overall cost of the generation can be formulated as below:

$$C_T = \sum_{i=1}^{N_G} C_{Pi} \quad (15)$$

As per the Siemens AG database the cost function of SVC and TCSC can be given as [21] :

$$C_{SVC} = (0.0003S^2 - 0.3051S + 127.38) * 88.2 \quad \$/kVAr \quad (16)$$

$$C_{tcsc} = (0.0015S^2 - 0.7130S + 153.75) * 88.2 \quad \$/KVAr \quad (17)$$

$$C_{FACTS} = C_{SVC} + C_{tcsc} \quad (18)$$

The objective function can be expressed as:

$$f_1 = C_{total} = \min(C_T + C_{FACTS}) \quad (19)$$

The primary ill effect of congestion in the system is the undesirable alteration of the voltage profile. Therefore, the next objective aims to curtail the voltage deviation of the system, which can be outlined as follows:

$$f_2 = Min D_v = \sum_n^{N_B} |V_n - V_{ref}|^2 \quad (20)$$

In Equation 20, D_v represents voltage deviation. V_n is the voltages at bus m and V_{ref} is the reference voltage. NB represents the total count of buses within the system. Power

loss in the transmission lines is another severe ill effect of congestion in the power system. These losses can be presented as:

$$Pl_{(m,n)} = g_{m,n} \{ (V_m - V_n)^2 + V_m V_n (\theta_m - \theta_n)^2 \} \quad (21)$$

In Equation 21, $Pl_{(m,n)}$ is the power loss in the line between bus m and bus n , V_m and V_n are the corresponding bus voltages, θ_m and θ_n are voltage angles at bus m and bus n , respectively, $g_{m,n}$ is the conductance of line k between bus m and bus n .

The multi-objective function can now be written as:

$$f = \min(\alpha C_{total} + \beta D_v + \gamma Pl_{(m,n)}) \quad (22)$$

Subject to the following constraints:

4.1. Power Balance Constraint

$$\begin{cases} P_{gi} = V_i \{ \sum_{j=1}^n V_j [G_{ij} \cos(\delta_i - \delta_j)] + P_{di} \} \\ Q_{gi} = V_i \{ \sum_{j=1}^n V_j [G_{ij} \sin(\delta_i - \delta_j)] - B_{ij} \sin(\delta_i - \delta_j) \} + Q_{di} \end{cases} \quad (23)$$

In Equation 23 P_{gi} and Q_{gi} are active and reactive power respectively generated at i^{th} bus, P_{di} and Q_{di} presents the respective active and reactive power demands at i^{th} bus, G_{ij} and B_{ij} are the conductance and susceptance part of the n^{th} element Y_{ij} of the Y bus admittance matrix of the system.

4.2. Inequality Constraints

$$\left. \begin{aligned} P_{gi}^{min} &\leq P_{gi} \leq P_{gi}^{max} \\ Q_{gi}^{min} &\leq Q_{gi} \leq Q_{gi}^{max} \\ V_i^{min} &\leq V_i \leq V_i^{max} \\ V_{gi}^{min} &\leq V_{gi} \leq V_{gi}^{max} \\ Q_{i,SVC}^{min} &\leq Q_{i,SVC} \leq Q_{i,SVC}^{max} \end{aligned} \right\} \quad (24)$$

The generated active power, denoted as, P_{gi} and reactive power, denoted as, Q_{gi} must fall within the specified range of acceptable minimum and maximum values. Similarly, for the power system to perform stable operation, the bus voltages, V_i and V_{gi} must lie between prescribed limits. $Q_{i,svc}$ represents the reactive power compensated by i^{th} SVC and it should lie between prescribed limits. Similarly, the generator's active power, P_{gi} , and the generated reactive power, Q_{gi} , must lie in the pre-specified maximum and minimum values. In addition, for reliable operation of the power system, the bus voltage V_i and the generator terminal voltage V_{gi} must also be within predetermined limits. Moreover, it is crucial that the i^{th} SVC effectively regulates the reactive power $Q_{i,svc}$ within the specified limits imposed on it. In general:

- 1) $V_{i,limits} = (0.90 \text{ pu}, 1.1 \text{ pu})$
- 2) $V_{gi,limits} = (0.95 \text{ pu}, 1.1 \text{ pu})$
- 3) $Q_{SVC,limits} = (-80 \text{ MVar}, 80 \text{ MVar})$

5. Results and Discussion

The proposed approach has been tested and verified using the IEEE 30 bus system, as depicted in Figure 3; this system has 30 buses and 41 lines. The state of deregulation is simulated by intentionally creating an outage of line number 12, which is between bus 6 and bus 10. This created N-1 contingency in the system under study.

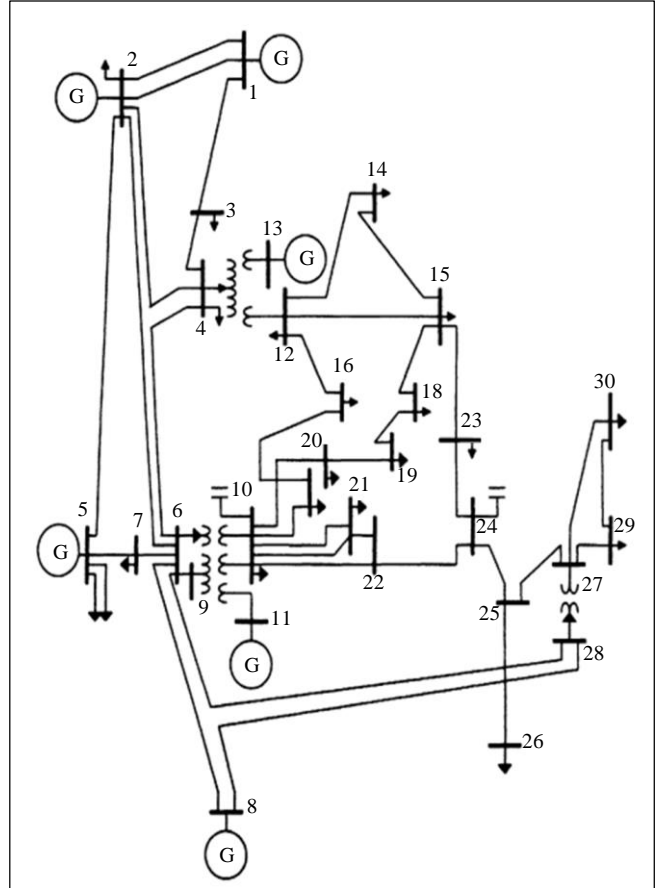


Fig. 3 IEEE 30 bus system

5.1. Voltage Deviation

The diagram in Figure 4 illustrates the change in the system's voltage profile after a congestion event. It's clear that the voltage profile of the system experiences a distortion when line number 12 is outed.

Utilizing the Grey Wolf Optimization (GWO) algorithm to improve the performance of SVCs at bus locations 3, 6, and 7 in the system has led to substantial improvements in the voltage profile. The initial voltage fluctuation of 0.01125 per unit (pu) that occurred when the network was congested has now been effectively decreased to 0.01058 pu. This significant enhancement has played a pivotal part in enhancing the overall stability of the system. To put it into perspective, the utilization of the GWO algorithm for optimizing SVC has resulted in an impressive reduction of 5.96% in voltage fluctuation across the entire system.

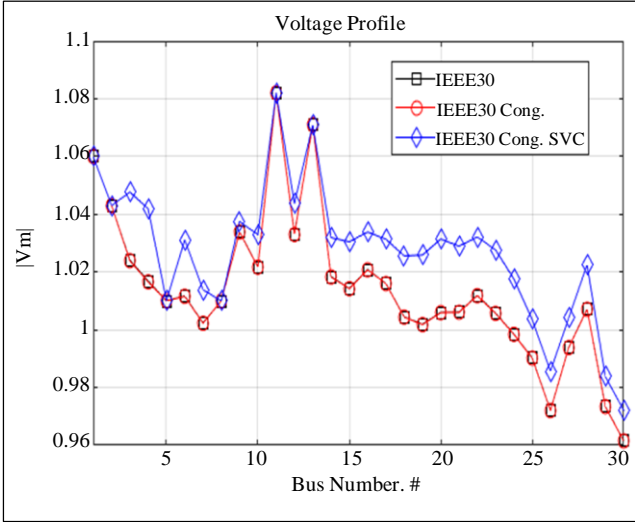


Fig. 4 Voltage profile of the system with GWO employing SVC



Fig. 5 Voltage profile of the system with TLBO employing SVC

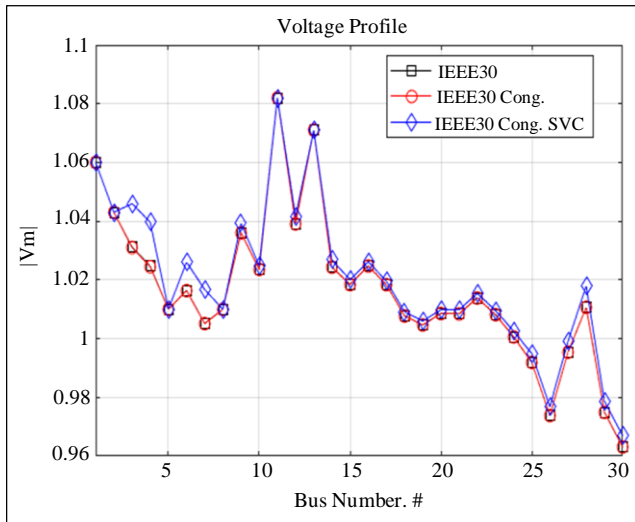


Fig. 6 Voltage profile of the system with GWO employing TCSC

Utilizing TLBO for optimization in both location and parameter tuning significantly improves the voltage profile, as depicted in Figure 5. It's important to emphasize that in this situation, there has been a significant improvement in the voltage profile. The deviation in voltage has been reduced noticeably, going from 0.01125 pu during congestion to a mere 0.01008 pu.

It can be seen that by using the TLBO method to implement SVC at bus numbers 3, 6, and 12, there has been a remarkable 10.4% decrease in voltage deviation. The voltage stability was also evaluated using the GWO method with the implementation of TCSC. Figure 6 displays the voltage patterns during congested situations caused by N-1 congestion and demonstrates the improved voltage pattern following the introduction of TCSC.

Noticeable improvements in the voltage performance are clearly visible after integrating TCSC into the system. The voltage fluctuation has been significantly reduced, dropping from 0.01125 pu during congestion to a mere 0.01110 pu. This positive change has been achieved by incorporating TCSC into transmission lines 3, 4, and 7, resulting in a remarkable 1.3% decrease.

This reduction has significantly enhanced the overall voltage stability of the congested system. When the TLBO algorithm is used to improve the performance of the TCSC, Figure 7 displays the resulting voltage profile in comparison to the voltage profile of the overloaded system.

Clearly, the use of the TLBO algorithm to optimize the TCSC results in a much more significant improvement in the voltage profile compared to when the TCSC is optimized using the GWO algorithm. To be more specific, in a congested system, the voltage deviation decreases to 0.011004 pu from the initial value of 0.01125 pu.

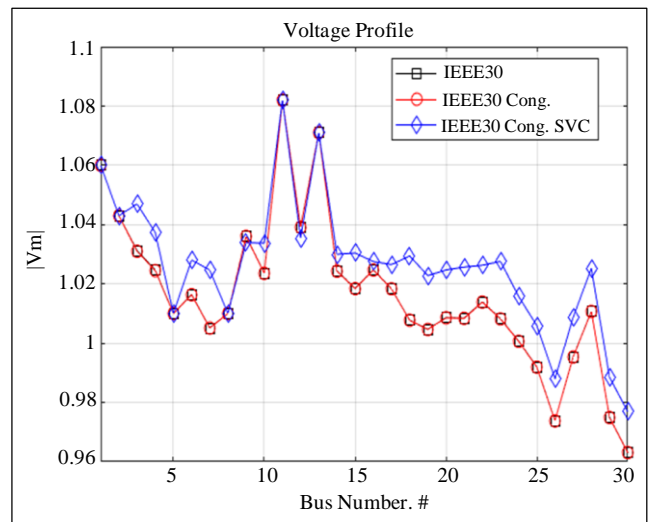


Fig. 7 Voltage profile of the system with TLBO employing TCSC

This represents a significant reduction of 2.186% in voltage deviation, achieved by employing the TLBO-optimized TCSC in the system. It's worth noting that the TCSC has been installed on line numbers 3, 6, and 15 in this scenario.

5.2. Power Loss

In Figure 8, we display the outcomes of optimizing the location and parameters of an SVC using GWO with the aim of reducing active power losses within the system. When a contingency situation arises and the SVC is not in operation, the total active power loss within the system amounts to 7.019 MW.

However, when we employ the GWO-optimized SVC, the active power loss decreases to 6.661 MW. Prior to the contingency, the power loss within the system was at 6.925 MW. As a result, implementing the SVC leads to a modest reduction in power loss. Additionally, it is noteworthy that in the most congested line (1), the MW loss is curbed from 5.155 MW to 1.268 MW. The SVC is now fine-tuned for both its location and parameters using the GWO technique. Figure 9 illustrates that the reactive power loss decreases from 69.2351 MVAR, as seen under contingency conditions, to 21.131 MVAR.

This represents a notable 50% reduction in reactive power loss. In the case of the most congested line, line number 1, the reactive power loss is substantially reduced from 15.46 MVAR in the congested case to a significant value of 3.8 MVAR. In Figure 10 and Figure 11, active power loss and reactive power loss reduction are presented, respectively, while TLBO is employed to obtain the location and parameter setting of SVC.

Now, the implementation of GWO for TCSC location and parameter optimization is being tested. Figures 12 and 13 represent the active power loss and reactive power loss reduction, respectively, when TCSC is optimized with GWO. In Figure 12, with the employment of TCSC, the MW loss is limited to 5.669 MW, which is less than the active power loss before congestion.

From Figure 13, it is clear that total reactive power loss is reduced to 22.41 MVAR, which is slightly higher than in the case of GWO optimized SVC but still is less than the reactive power loss before the congestion occurred. Figure 14 shows the outcomes of using TLBO to optimize the location and parameters of TCSC, which resulted in a reduction in active power loss. Specifically, under contingency conditions, the active power loss decreased from 7.019 MW to 3.440 MW. Furthermore, the active power loss on the congested line decreased from 5.155 MW to 1.7345 MW when TCSC was implemented. This implementation led to a notable 33.184% reduction in active power loss in this case.

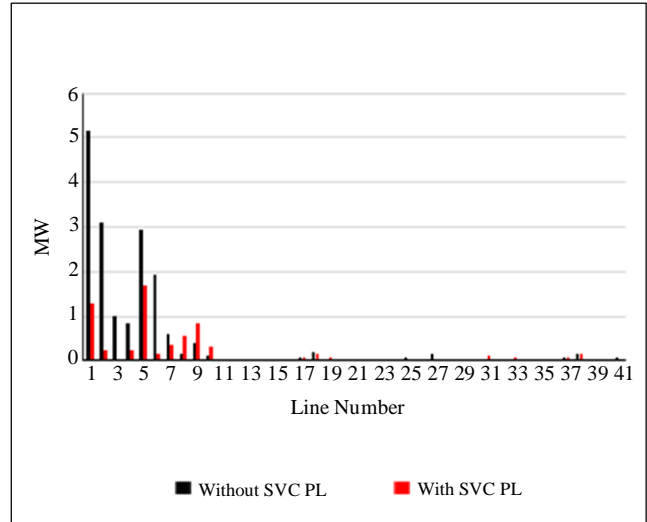


Fig. 8 Active power loss of the system with GWO employing SVC

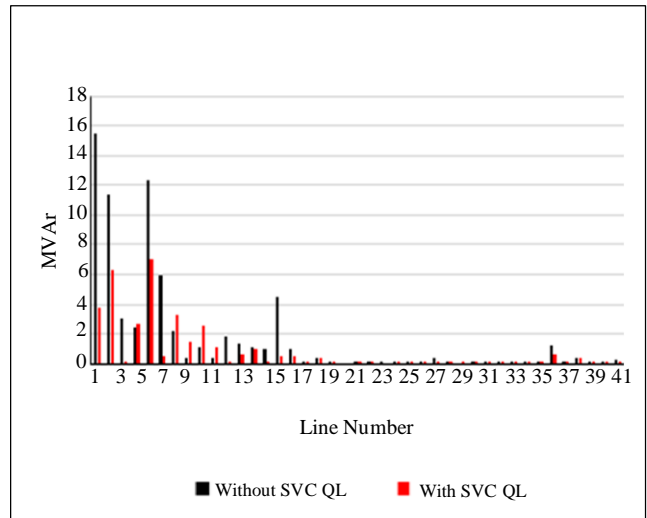


Fig. 9 Reactive power loss of the system with GWO employing SVC

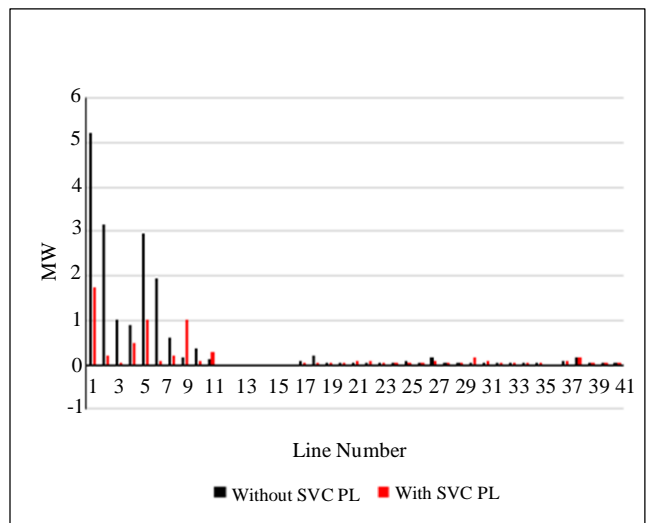


Fig. 10 Active power loss of the system with TLBO employing SVC

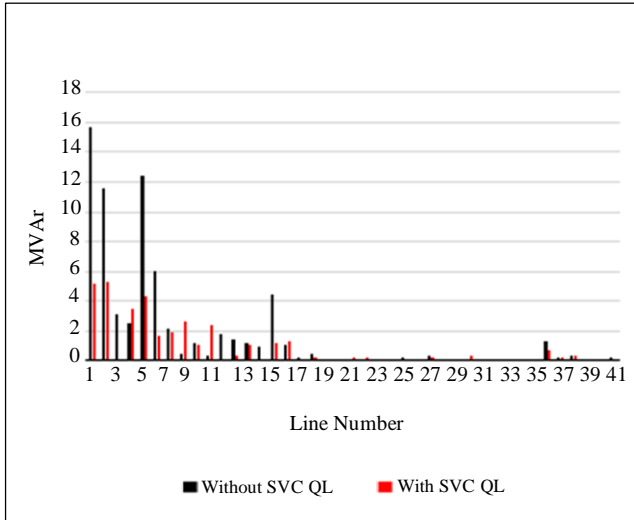


Fig. 11 Reactive power loss of the system with TLBO employing SVC

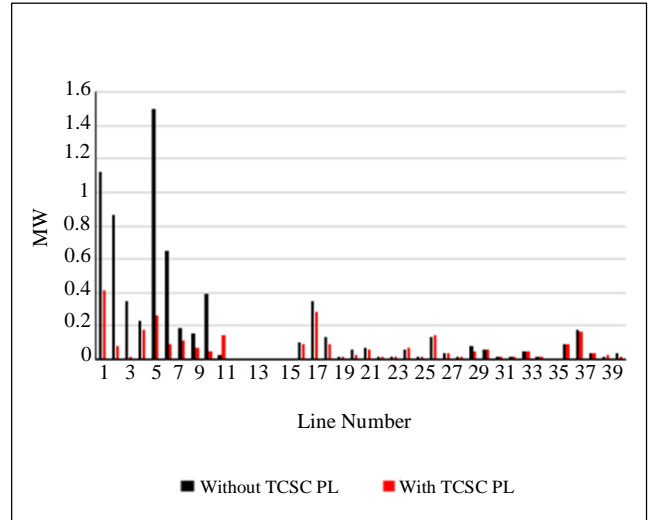


Fig. 14 Active power loss of the system with TLBO employing TCSC

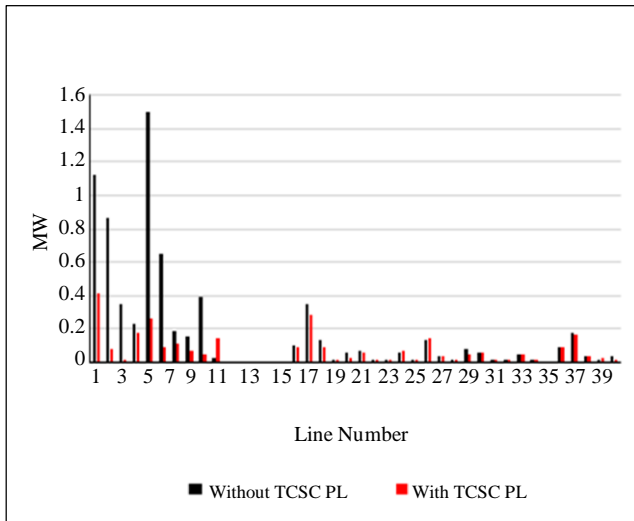


Fig. 12 Active power loss of the system with GWO employing TCSC

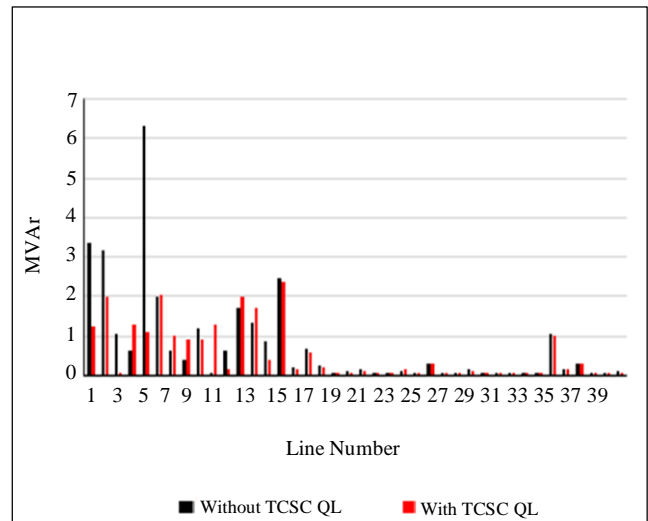


Fig. 15 Reactive power loss of the system with TLBO - TCSC

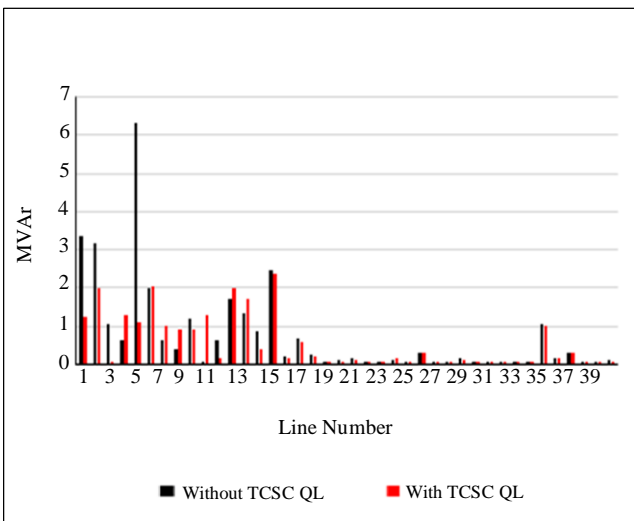


Fig. 13 Reactive power loss of the system with GWO employing TCSC

Optimizing TCSC using TLBO results in a substantial decrease in reactive power loss. Specifically, the loss is reduced from 69.2351 MVar to 34.8859 MVar when the power system is congested. This reduction is clearly illustrated in Figure 15. Additionally, it's worth noting that the reactive power loss in congested transmission lines also experiences a significant decrease. The consolidated comparison of the results obtained for power loss reduction by implementing SVC and TCSC employing GWO and TLBO are presented in Table 1. Table 1 shows that the TLBO-optimized SVC reduces the active power loss by 6.227 MW as compared to GWO-optimized SVC, which diminishes the actual power loss to 6.7265 MW. When TLBO optimizes TCSC, the actual power loss is limited significantly to 3.440 MW, which is much better than GWO-optimized TCSC, which reduces MW loss to 7.1986 MW. These results justify the supremacy of TLBO over GWO.

Table 1. Consolidated results for power loss reduction employing GWO and TLBO

FACTS	Optimization Methods			
	GWO		TLBO (Proposed)	
	SVC	TCSC	SVC	TCSC
Active Power Loss (MW)	6.7265 [22]	7.1986 [22]	6.2268	3.440
Reactive Power Loss (MVar)	21.131	22.41	34.25	34.88

Table 2. Consolidated results for generation cost reduction and location of FACTS devices

FACTS	Optimization Methods			
	GWO		TLBO (Proposed)	
	SVC	TCSC	SVC	TCSC
Generation Cost (\$/hr)	837.043	830.809	835.3195	824.1284
Device Cost (\$/hr)	36.0153	25.1532	25.36145	24.35687
Total Cost (\$/hr)	873.058	855.962	860.6810	848.4853
Location	Bus No. (3,6,7)	Line No. (3,4,7)	Bus No. (3,6,12)	Line No. (3,6,15)
Voltage Deviation (pu)	0.01058	0.0111	0.01008	0.011004

5.3. Generation Cost

The decrease in generation expenses resulting from the use of both SVC and TCSC has been computed. Table 1 presents a detailed summary of the outcomes, illustrating the reduction in generation costs attained by utilizing SVC and TCSC, along with the corresponding algorithms. Before the introduction of FACTS devices to alleviate congestion, the generation cost was 880.212 \$ per hour.

It’s important to note that when we use the GWO-optimized SVC and TCSC, we see a significant decrease in voltage deviation: 5.96% for SVC and 1.3% for TCSC. However, when we apply the TLBO algorithm to optimize SVC and TCSC, the reduction in voltage deviation is even more substantial, reaching 10.4% for SVC and 2.180% for TCSC.

This observation highlights that optimizing the placement and settings of SVC leads to much lower voltage deviations compared to TCSC. Clearly, when it comes to reducing voltage deviation, TLBO-optimized SVC performs better than GWO. To provide a more comprehensive picture, we have analyzed the costs associated with generators, equipment, and overall expenses in the generation process, as shown in Table 2.

The results indicate that when GWO-optimized SVC is employed, the total generation cost is \$873.058 per hour. This cost includes a generation cost of \$837.04343 per hour and an additional SVC cost of \$36.0153 per hour. Additionally, when we examine the overall costs of power generation, we find that the GWO-optimized TCSC system costs \$855.96243 per hour, the TLBO-optimized SVC system costs \$860.68103 per hour, and the TLBO-optimized TCSC system costs \$848.48533 per hour.

These numbers clearly indicate that TCSC is more efficient than SVC in reducing generation costs. Notably, when TLBO optimization is applied to TCSC, it achieves the most significant reduction in total generation costs, outperforming GWO optimization. Figure 16 provides a summary of how the objective function is minimized for cost reduction.

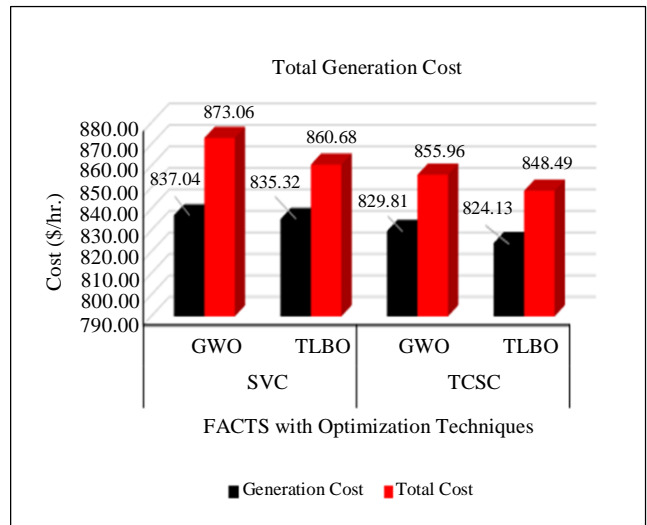


Fig. 16 Minimization of the objective function

5. Conclusion

In this research paper, we investigate the use of shunt FACTS device SVC and series FACTS device TCSC in the IEEE 30 bus system with the primary goal of reducing the operational expenses of generators. The stability and dependability of an electrical power system rely significantly on maintaining voltage levels within specified limits. In this study, we have successfully applied SVC and TCSC to

reduce voltage deviations and alleviate congestion in the system. Notably, the utilization of TLBO optimization for SVC has led to a noteworthy decrease in voltage deviations and reactive power losses. This improvement is a result of injecting reactive power at specific locations, resulting in an enhanced voltage profile. Conversely, when TCSC is incorporated into the system, it leads to significant reductions

in generation costs, cutbacks in active power losses, and decreased operational expenses associated with FACTS devices. The applied TLBO algorithm-optimized SVC proves highly efficient in minimizing voltage deviations and reactive power losses. At the same time, TLBO-optimized TCSC effectively reduces overall generation costs and active power losses in the system.

References

- [1] Anurag Gautam et al., "Methods and Methodologies for Congestion Alleviation in the DPS: A Comprehensive Review," *Energies*, vol. 16, no. 4, pp. 1-28, 2023. [[CrossRef](#)] [[Google Scholar](#)] [[Publisher Link](#)]
- [2] S. Surender Reddy, "Optimal Placement of FACTS Controllers for Congestion Management in the Deregulated Power System," *International Journal of Electrical and Computer Engineering (IJECE)*, vol. 8, no. 3, pp. 1336-1344, 2018. [[CrossRef](#)] [[Google Scholar](#)] [[Publisher Link](#)]
- [3] Anwar S. Siddiqui, and Tanmoy Deb, "Congestion Management Using FACTS Devices," *International Journal of System Assurance Engineering and Management*, vol. 5, no. 4, pp. 618-627, 2014. [[CrossRef](#)] [[Google Scholar](#)] [[Publisher Link](#)]
- [4] Yogasree Manganuri et al., "Optimal Location of TCSC Using Sensitivity and Stability Indices for Reduction in Losses and Improving the Voltage Profile," *2016 IEEE 1st International Conference on Power Electronics, Intelligent Control and Energy Systems (ICPEICES)*, Delhi, India, pp. 1-4, 2016. [[CrossRef](#)] [[Google Scholar](#)] [[Publisher Link](#)]
- [5] Sai Ram Inkollu, and Venkata Reddy Kota, "Optimal Setting of FACTS Devices for Voltage Stability Improvement Using PSO Adaptive GSA Hybrid Algorithm," *Engineering Science and Technology, an International Journal*, vol. 19, no. 3, pp. 1166-1176, 2016. [[CrossRef](#)] [[Google Scholar](#)] [[Publisher Link](#)]
- [6] S.N. Singh, and A.K. David, "Optimal Location of FACTS Devices for Congestion Management," *Electric Power Systems Research*, vol. 58, no. 2, pp. 71-79, 2001. [[CrossRef](#)] [[Google Scholar](#)] [[Publisher Link](#)]
- [7] Divya Gupta, and Sanjay Kumar Jain, "Available Transfer Capability Enhancement by FACTS Devices Using Metaheuristic Evolutionary Particle Swarm Optimization (MEEPSO) Technique," *Energies*, vol. 14, no. 4, pp. 1-28, 2021. [[CrossRef](#)] [[Google Scholar](#)] [[Publisher Link](#)]
- [8] Hossein Hashemzadeh, and Seyed Hamid Hosseini, "Locating Series FACTS Devices Using Line Outage Sensitivity Factors and Particle Swarm Optimization for Congestion Management," *2009 IEEE Power & Energy Society General Meeting*, Calgary, Canada, pp. 1-6, 2009. [[CrossRef](#)] [[Google Scholar](#)] [[Publisher Link](#)]
- [9] K. Vijayakumar, "Optimal Location of FACTS Devices for Congestion Management in Deregulated Power Systems," *International Journal of Computer Applications*, vol. 16, no. 6, pp. 29-37, 2011. [[CrossRef](#)] [[Google Scholar](#)] [[Publisher Link](#)]
- [10] Naresh Acharya, and N. Mithulananthan, "Locating Series FACTS Devices for Congestion Management in Deregulated Electricity Markets," *Electric Power Systems Research*, vol. 77, no. 3-4, pp. 352-360, 2007. [[CrossRef](#)] [[Google Scholar](#)] [[Publisher Link](#)]
- [11] Manasarani Mandala, and C.P. Gupta, "Congestion Management by Optimal Placement of FACTS Device," *2010 Joint International Conference on Power Electronics, Drives and Energy Systems & 2010 Power India*, New Delhi, India, pp. 1-7, 2010. [[CrossRef](#)] [[Google Scholar](#)] [[Publisher Link](#)]
- [12] Anwar Shahzad Siddiqui, Mohd Tauseef Khan, and Fahad Iqbal, "Determination of Optimal Location of TCSC and STATCOM for Congestion Management in Deregulated Power System," *International Journal of System Assurance Engineering and Management*, vol. 8, pp. 110-117, 2017. [[CrossRef](#)] [[Google Scholar](#)] [[Publisher Link](#)]
- [13] Akash Sharma, and Rajive Tiwari, "Voltage Profile Enhancement Using FACTS Devices," *Intelligent Computing Techniques for Smart Energy Systems*, pp. 119-132, 2022. [[CrossRef](#)] [[Google Scholar](#)] [[Publisher Link](#)]
- [14] Arun Kumar Reddy K., and Shiv P. Singh, "Congestion Mitigation Using UPFC," *IET Generation, Transmission & Distribution*, vol. 10, no. 10, pp. 2433-2442, 2016. [[CrossRef](#)] [[Google Scholar](#)] [[Publisher Link](#)]
- [15] Akanksha Mishra, and G. Venkata Nagesh Kumar, "Congestion Management of Deregulated Power Systems by Optimal Setting of Interline Power Flow Controller Using Gravitational Search Algorithm," *Journal of Electrical Systems and Information Technology*, vol. 4, no. 1, pp. 198-212, 2017. [[CrossRef](#)] [[Google Scholar](#)] [[Publisher Link](#)]
- [16] K. Bavithra, S. Charles Raja, and P. Venkatesh, "Optimal Setting of FACTS Devices Using Particle Swarm Optimization for ATC Enhancement in Deregulated Power System," *IFAC-PapersOnLine*, vol. 49, no. 1, pp. 450-455, 2016. [[CrossRef](#)] [[Google Scholar](#)] [[Publisher Link](#)]
- [17] B. Chong et al., "Optimal Location of Unified Power Flow Controller for Congestion Management," *European Transactions on Electrical Power*, vol. 20, no. 5, pp. 600-610, 2009. [[CrossRef](#)] [[Google Scholar](#)] [[Publisher Link](#)]

- [18] A.Vengadesan, "Transmission Congestion Management through Optimal Placement and Sizing of TCSC Devices in a Deregulated Power Network," *Turkish Journal of Computer and Mathematics Education*, vol. 12, no. 6, pp. 5390-5403, 2021. [[Google Scholar](#)] [[Publisher Link](#)]
- [19] Debasish Mondal, Abhijit Chakrabarti, and Aparajita Sengupta, "Application of FACTS Controller," *Power System Small Signal Stability Analysis and Control*, pp. 197-242, 2020. [[Google Scholar](#)]
- [20] R.V. Rao, V.J. Savsani, and D.P. Vakharia, "Teaching-Learning-Based Optimization: A Novel Method for Constrained Mechanical Design Optimization Problems," *Computer-Aided Design*, vol. 43, no. 3, pp. 303-315, 2011. [[CrossRef](#)] [[Google Scholar](#)] [[Publisher Link](#)]
- [21] L.J. Cai, I. Erlich, and G. Stamtsis, "Optimal Choice and Allocation of FACTS Devices in Deregulated Electricity Market Using Genetic Algorithms," *IEEE PES Power Systems Conference and Exposition*, New York, USA, vol. 1, pp. 201-207, 2004. [[CrossRef](#)] [[Google Scholar](#)] [[Publisher Link](#)]
- [22] Ahmed A. Shehata et al., "Power System Operation Enhancement Using A New Hybrid Methodology for Optimal Allocation of FACTS Devices," *Energy Reports*, vol. 8, pp. 217-238, 2022. [[CrossRef](#)] [[Google Scholar](#)] [[Publisher Link](#)]